IJCRT.ORG ISSN : 2320-2882

INTERNATIONAL JOURNAL OF CREATIVE RESEARCH THOUGHTS (IJCRT)

An International Open Access, Peer-reviewed, Refereed Journal

Exploring Structural and Morphological Properties of Self-Propagating Auto-Combusted $Ni_{1-X}Zn_xFe_2O_4$ Ferrites

[1] A.S. Jagdale, [*2] D.H. Bobade, [3] B. Ghule

[1]Research Scholar, [*2]Associate Professor, [3]Assistant Professor

[1] Department of Physics, Ahmednagar College, Ahilyanagar , SPPU,Pune, (M.S.), India

[*2]C.T. Bora College, Shirur, Pune, SPPU,Pune ,(M.S.), India,

[3]School of Engineering & Technology, D Y Patil University Pune, Ambi, Pune, (M.S.), India

Abstract: Nickel–zinc ferrites are the magnetic materials that shows diverse industrial applications especially in the photo catalysis owing to their magnetic coactivity and eddy current loss with low value electrical resistivity with high value that affects and tailor these soft magnetic nano ferrites structural and morphological characteristics. In existing study, we have synthesized zinc doped nickel ferrites Ni1-xZnxFe2O4 nanoparticles (NPs) with variation in nickel and zinc concentration simultaneously as (x = 0.0, 0.2, 0.4, 0.6 ,0.8,1.0)) via Sol-Gel auto combustion technique.

The structural analysis of the NPs was carried out by XRD technique. We compare our results with JCPDS #01-073-1963. From this study we conclude that the synthesized NPs are cubic spinel structure with preferential orientation along the (311) plane. D-spacing for (311) plane varies from 2.48 to 2.53 **A^0.** We have determined the crystallite size using the Debay-Scherer Formula and we observed crystallite size in between the 22nm to 29nm. Investigations by XRD revealed that all the prepared samples demonstrate a pure phase. Alterations in the lattice parameters and micro-strain observed due to introduction of Zn in the crystal structure. Morphology of the synthesized NPs analyzed using the FESEM. We have observed that synthesized NPs are porous in nature. With concentration of nickel and zinc, this porosity varies. Stoichiometry of the NPs was studied with the help of EDS spectra. It confirms the presence of the nickel, zinc, iron and oxygen in the NPs. With change in the concentration, we observed the variation in the atomic % of Zinc and Nickel.

Keywords-Nickel–zinc ferrites; FESEM; nanoparticles; XRD; EDS; Sol-gel Method

1. INTRODUCTION

In the last few decades, magnetic spinel ferrites have much more attention due to their quantum confinement effect which was depends on their remarkable structural, morphological proprieties that gives versatile applications such as memory devices, high frequency devices, charge storage devices, gas sensors, photocatalysis, water splitting. For these applications there is necessity of high densities, low porosity and specific surface to volume ratio, microstructures [1, 2, 3]. This was specially depending on structure of spinel ferrites that have general formula AFe_2O_4 where, 'A' represents divalent metal cations i.e., $Mg^{2+,}$ Ni^{2+}, Co^{2+}, Zn^{2+} etc. It having FCC structure of anions of oxygen and its every unit cell contains tetrahedral 64-A sites and octahedral 32- sites [4]. There are two types of spinel ferrites depending upon distribution of cations A^{2+} and Fe^{3+} on the sites [A] or [B]. AB_2O_4 is the normal spinel type having formula $(A^{2+})_A[Fe^{3+}Fe^{3+}]_BO^{2-}$ and $B(AB)O_4$ is the inverse spinel type having formula $(A^{2+}Fe^{3+})_A[A^{2+}Fe^{3+}]_BO^{2-}$.

As shown in Fig. 1. (Fig. 1 is adopted from open access article [5]) spinel ferrites form by the ions of metals gets trapped by the void space of oxygen ions due to its smaller ionic radius than that of ionic radius of oxygen.

The presence of cations on the residence of cations [A] and [B] sites gives remarkable changes in the magnetic and structural properties of these spinel ferrites [5].

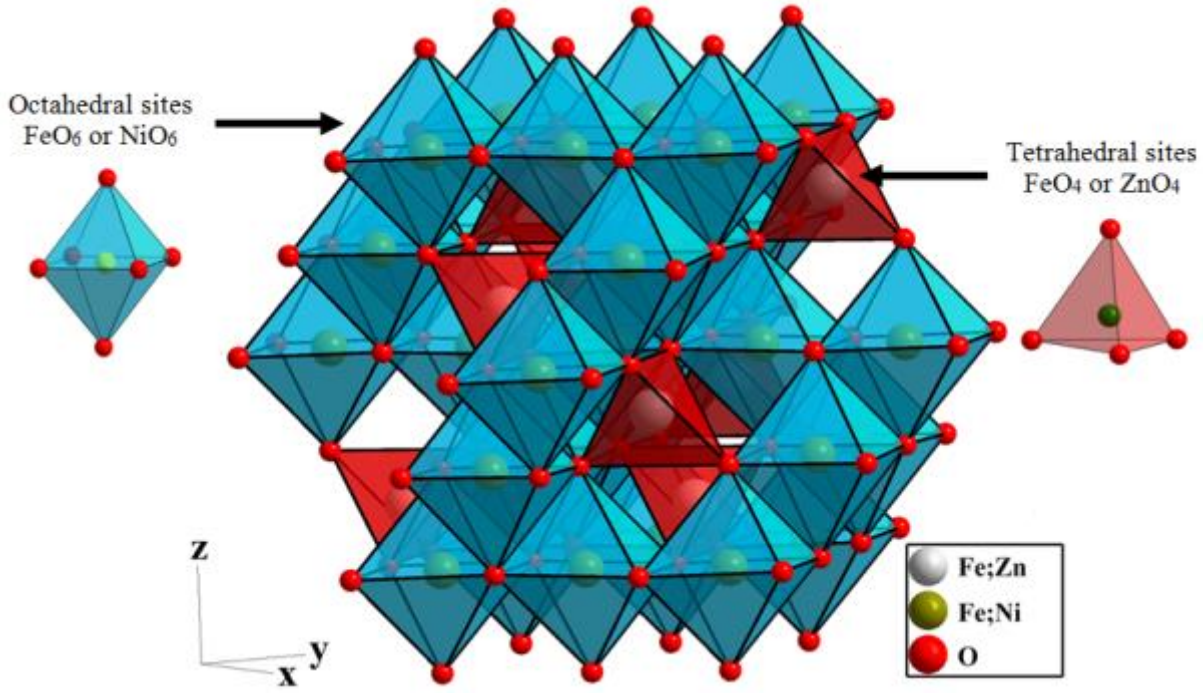

Figure 1: Spinnel Ferrite Structure [5]

In the bulk form of nickel-Zinc ferrites, generally tetrahedral position occupied by Zn ions and octahedral positions occupied by nickel ions. But it was also found that in the nanocrystalline form the small percentage of nickel and zinc ions can be occupying tetrahedral and octahedral positions correspondingly [6,7]. The morphological and magnetic properties of spinel nano ferrites get affected by methods of preparation, doping element and its composition that helps to improve their applications in different fields. $Ni_xZn_{1-x}Fe_2O_4$ turn out to be an important soft magnetic ferrites materials owing to their greater resistivity and saturation magnetization also their coercivity with low value in between the other transition metal ferrite materials, i.e. (MFe_2O_4) [8,9]. It's variety of applications in different areas of science and technology like antenna, EMI suppress, transformer cores, memory devices, sensors technology, magnetic heads of multiple path communications, catalytic applications, supercapacitor, water splitting, energy storage devices and in the gas sensing applications [10,11,12].

The reported work represents the zinc doped nickel ferrites nanoparticles using sol-gel auto combustion method. This auto combustion method has found to be noticeable choice for the ferrites nanoparticles synthesis because of is advantageous parameters such as good stoichiometric control, efficient production of nanoparticles, less expensive, exothermic reaction with the release of more heat rate, good crystallinity, high yield, simple and easy method of synthesis of nanoparticles [13,14].

In this paper we reported that effect of Zn doping in nickel ferrite by studying their morphological, structural and optical properties because of doping of Zn which is non-magnetic ion is expected to alter the properties by varying the cation distribution in between two crystallographic sites such as A and B-sites i.e. octahedral and tetrahedral sites of cubic spinel ferrites. The variation in Zn and Ni as $Ni_{1-x}Zn_xFe_2O_4$ (x = 0.0, 0.2, 0.4, 0.6, 0.8, 1.0) nanoparticles synthesized via sol-gel method in the current investigation that structural properties by XRD technique, morphological properties and elemental composition by using FESEM with EDS technique.

2. Experimental:

In this reported work**,** $Ni_{1-x}Zn_xFe_2O_4$ (x = 0.0, 0.2, 0.4, 0.6, 0.8, 1.0)) nanoparticles were synthesized by a sol-gel method. Stoichiometric amount of ferric nitrate hexahydrate, nickel nitrate hexahydrate, citric acid, zinc nitrate hexahydrate was used as precursor and dissolve in double distilled water using continuous stirring by using magnetic stirrer. By adding drop by drop ammonia the pH of solution maintains 7 i. e. neutral. This homogeneous mixture was continuously stirring and heated at constant temperature 80^0C using magnetic stirrer until the gel formation [2]. In this process hydrolysis followed by condensation there is formation of gel is there. After that sudden increase in temperature causes process of auto combustion with liberation of gases N_2 and CO_2 so there is production of foamy, voluminous fine brownish coloured $Ni_{1-x}Zn_xFe_2O_4$ samples. The synthesized sample was grinded using pestle and mortar to make fine powder form and then annealed at temperature 500 ^{0}C for 4Hrs. in muffle furnace. The synthesized samples of $Ni_{1-x}Zn_xFe_2O_4$ series

like $Ni_{1.0}$ $Zn_{0.0}Fe_2O_4$, $Ni_{0.8}$ $Zn_{0.2}Fe_2O_4$, $Ni_{0.6}$ $Zn_{0.4}Fe_2O_4$, $Ni_{0.4}$ $Zn_{0.6}Fe_2O_4$, $Ni_{0.2}$ $Zn_{0.8}Fe_2O_4$ and $Ni_{0.0}$ $Zn_{1.0}Fe_2O_4$ were labeled as A1, B1, C1, D1, E1, F1 correspondingly. Fig. 2 shows process of synthesis of $Ni_{1-x}Zn_xFe_2O_4$ NPs by sol-gel method.

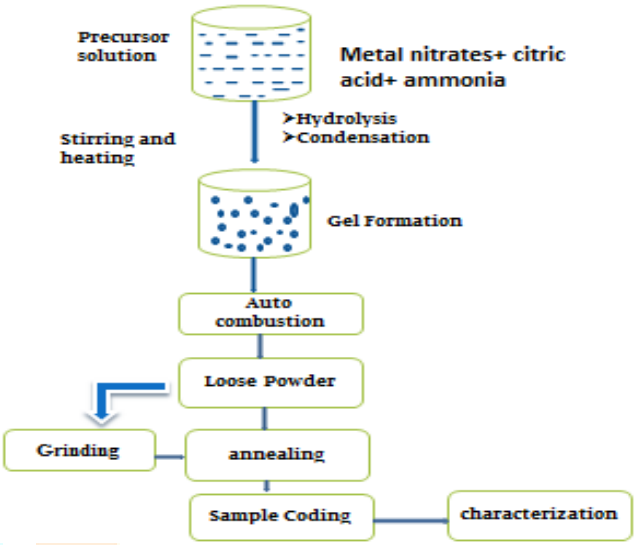

Fig. 2. Flowchart of synthesis of $Ni_{1-x}Zn_xFe_2O_4$ NPs by sol-gel method

3. Characterization:

Prepared samples were further used to study structural, optical properties by using different characterization techniques. The XRD patterns were recorded in the 2**θ** range of 10-80^0 using Cu-K**α** radiation (**λ**=1.5405Å) using Bruker XRD model. Using field emission scanning electron microscope (FESEM) by using JEOL-JSM 840 model operating on 2.131 keV. Morphological study and elemental analysis of synthesized samples has been done.

4. Results and discussion:

4.1: X-ray diffraction studies:

XRD graphs of synthesized $Ni_{1-x}Zn_xFe_2O_4$ ferrites by sol-gel method are shown in following fig.3. The XRD patterns confirms that synthesized samples consist of crystalline structures of FCC spinel ferrites with fd-3m space group of symmetry. Observed sharp peaks in XRD pattern indicates that there is good crystallization of the products. There was no observed peak of impurity in the XRD spectra that gives confirmation of the pure ferrite phase. The XRD pattern shows the strong reflection's namely (111), (220), (311), (400), (422), (511) and (440). The detected diffraction peaks consistent with JCPDS Data Card JCPDS # 01-073-1963 that confirms for cubic spinel structure of synthesized NPs. Crystallite size was examine by most intense peak (311) in XRD pattern using Debay Scherrer equation, $D = \frac{0.9\lambda}{\beta cos\theta}$, where **θ** is the Bragg's angle, **λ** is the x-rays wavelength, **β** is the full width and half maxima measure in radians [4] .The average crystallite sizes calculated are 26.09, 26.89, 22.55, 23.32, 23.45 and 23.99 nm for x= 0.0, 0.2, 0.4, 0.6, 0.8, 1.0 respectively. The observed crystallite size varied in between the 22nm to 29nm.

Investigations by X-ray diffraction revealed that all samples of ferrites demonstrate a pure phase. Modifications in the lattice parameters and micro-strain observed due to introduction of Zn in the crystal structure of prepared samples. It was found that d-spacing for (311) plane varies from 25.28nm to 24.79 nm with the change in concentration of Zn. Also, d-spacing for (400) plane varies from 14.87nm to 14.63nm with the change in concentration of Zn. Figure.2. illustrates that lower angle shifting of diffraction peaks observed when Zn concentration increases. This is because of there is replacement of larger Zn^{2+} cations in smaller Ni^{2+} cation. Also, maximum intensity of peak was observed for (311) plane showed that grains of nanoparticles were dominating [4].

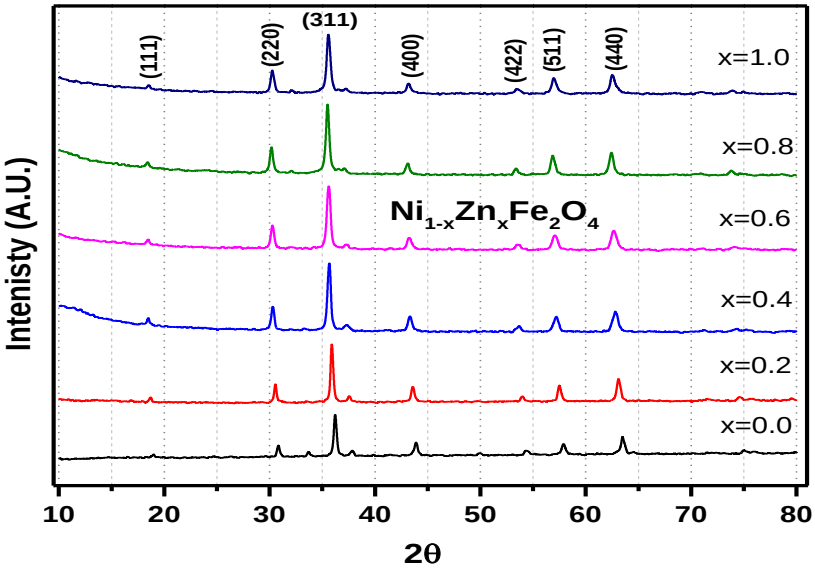

Fig.3. X-ray diffraction pattern of $Ni_{1-x}Zn_xFe_2O_4$ ferrites

The lattice parameter a calculated by using relation, $a = \frac{d}{\sqrt{(h^2+k^2+l^2)}}$ [4].

Where, inter planar distance (d) and Bragg's angle (2**θ**). It was observed that lattice parameter rises with the rise in Zn concentration this is because of there is replacement of larger Zn^{2+} cations in smaller Ni^{2+} cation [2].

Table.1. X-ray diffraction analysis of $Ni_{1-x}Zn_xFe_2O_4$ samples

Composition	d (311) (A^0)	d (400) (A^0)	a (311) (A^0)	a(400) (A^0)
$Ni_1Zn_{0.0}Fe_2O_4$	2.47980	2.06295	8.2236	8.2518
$Ni_{0.8}Zn_{0.2}Fe_2O_4$	2.50066	2.07620	8.2936	8.3048
$Ni_{0.6}Zn_{0.4}Fe_2O_4$	2.51853	2.08853	8.3529	8.3541
$Ni_{0.4}Zn_{0.6}Fe_2O_4$	2.52143	2.09174	8.3615	8.3669
$Ni_{0.2}Zn_{0.8}Fe_2O_4$	2.5224	2.09473	8.3657	8.3789
$Ni_{0.0}Zn_1Fe_2O_4$	2.5288	2.09935	8.3794	8.3974

The variation in the lattice parameter and interplanar spacing with respect to Zn^{2+} ion concentration is plotted in Fig 4.and Fig 5. The increasing trend of lattice parameter and interplanar spacing with the increase in Zn^{2+} ion attributed to larger atomic radii of Zn^{2+} ion than Ni^{2+} ion [6].

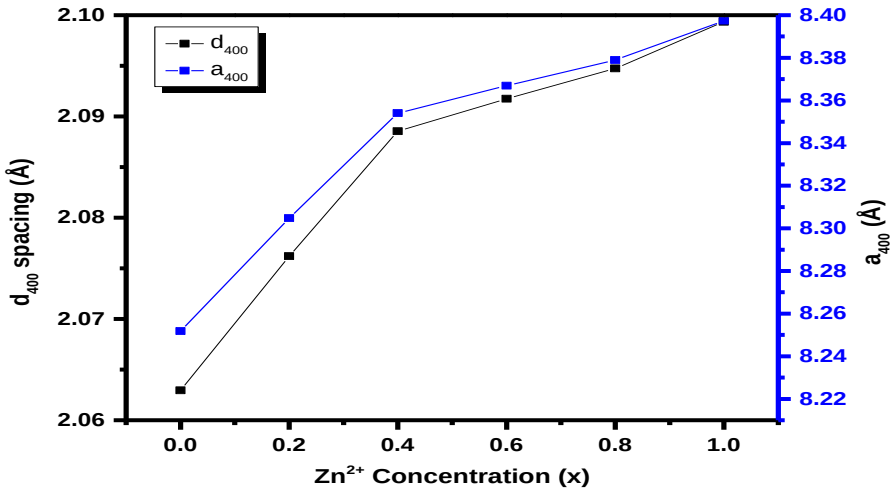

Fig. 4. Variation in d-spacing and lattice parameter for (400) plane

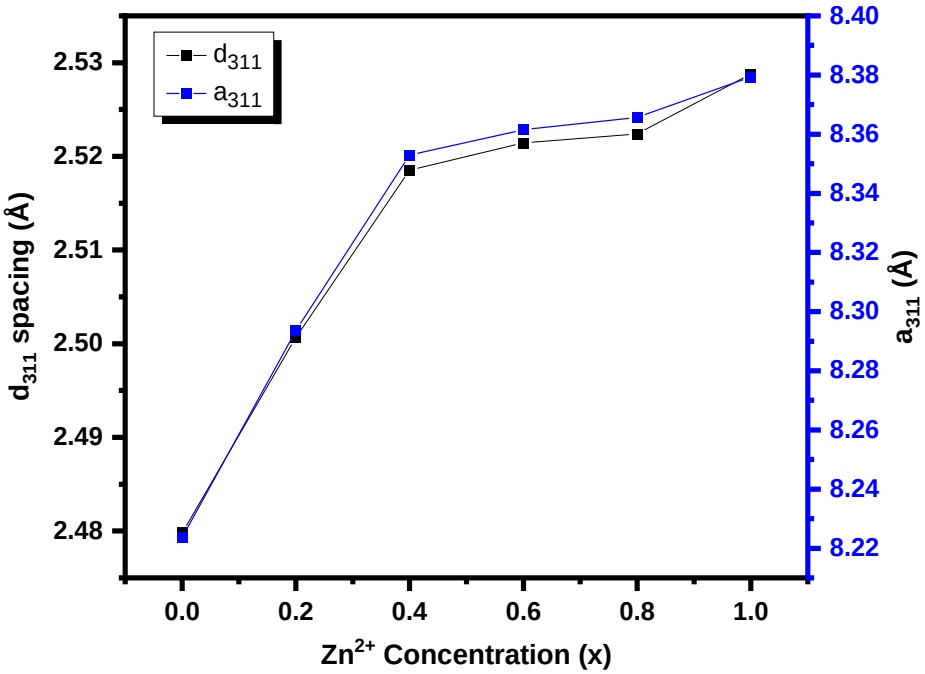

Fig. 5. Variation in d-spacing and lattice parameter for (311) plane

4.2.Morphological characterizations:

4.2.1. **FESEM studies**:

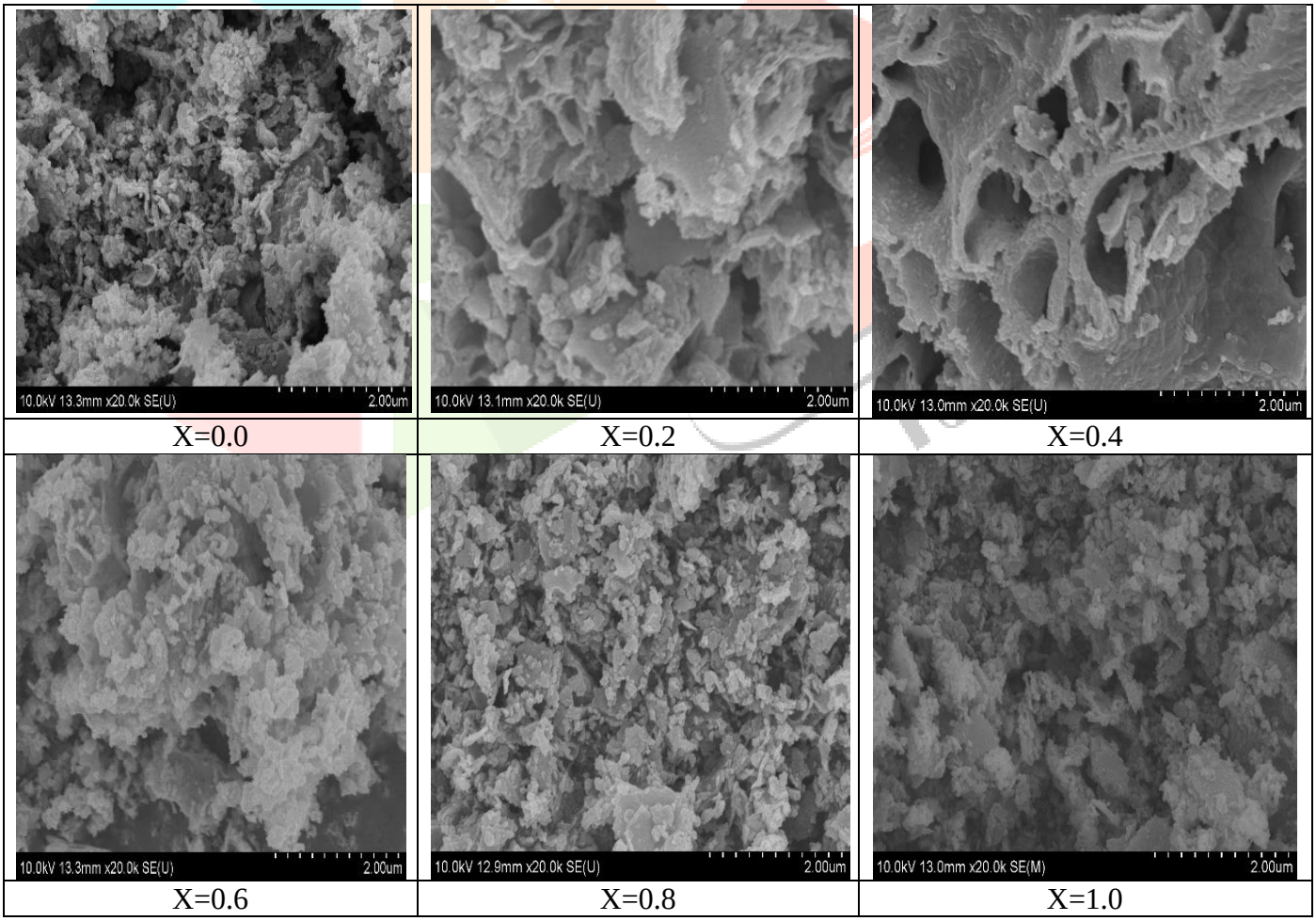

Fig.6. FESEM micrographs of $Ni_{1-x}Zn_xFe_2O_4$ nanoparticles

Morphology of the $Ni_{1-x}Zn_xFe_2O_4$ NPs has been studied using FESEM. Fig.6. indicates FESEM micrograph that shows the particles exhibit a tendency to agglomerate with sponge like morphology. This loosely agglomerated grains having porous nature because of during auto combustion process of synthesis

agglomeration are likely to be formed due to the release of huge quantity of gases during combustion process [15]. The agglomeration behavior of the NPs can be associated to the magnetic dipole-dipole interaction [9] It was observed that Zn substitution in Ni ferrite shows greatest influence on the microstructure, and the grain size of NPs. Synthesized NPs are porous in nature. With the increase in the concentration of zinc the nanoparticles become more irregular, corned and non-symmetric along with agglomeration happens.

4.2.2. EDS studies:

Investigation of elemental study done by using EDS spectra that shows strong peaks of Ni, Zn, Fe and O, confirming the presence of elements shown in fig. 7. In figure 7. the FESEM image shows the selected area for EDS study and corresponding EDS spectra. Table 2 shows the numerical values of weight & atomic percentage of elements present in synthesized nanoparticles.

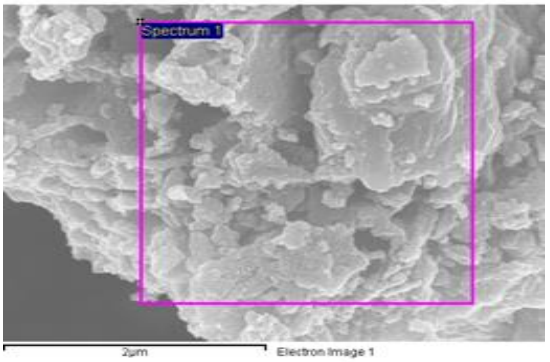

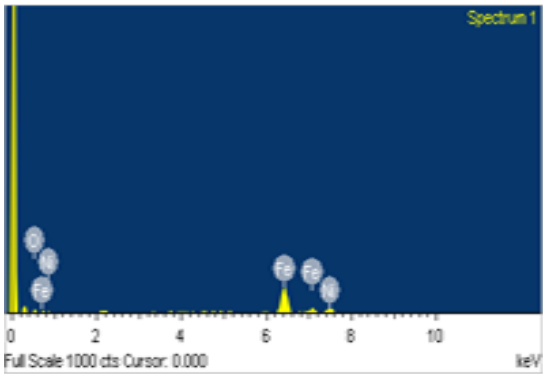

X=0.0

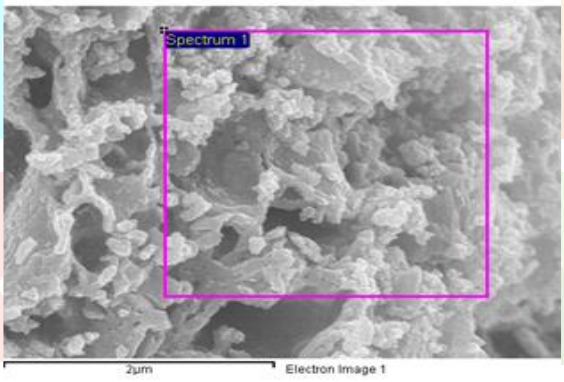

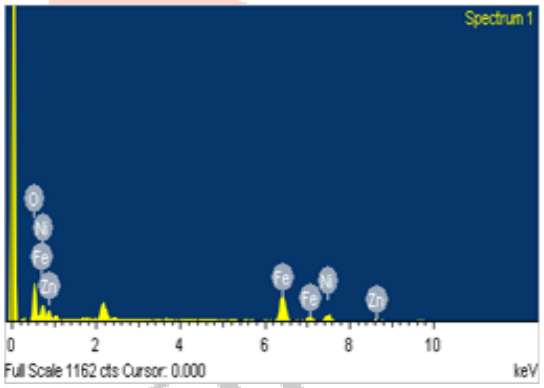

X=0.2

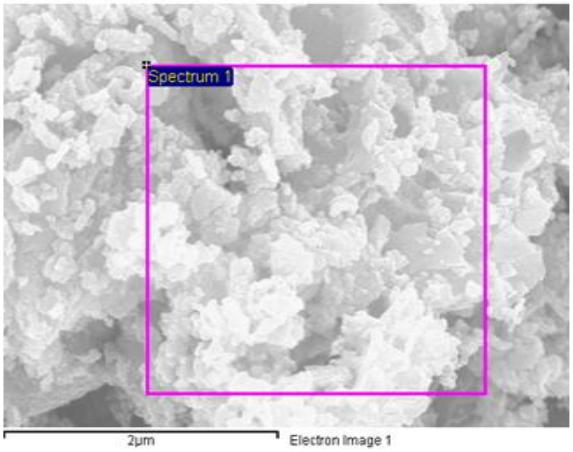

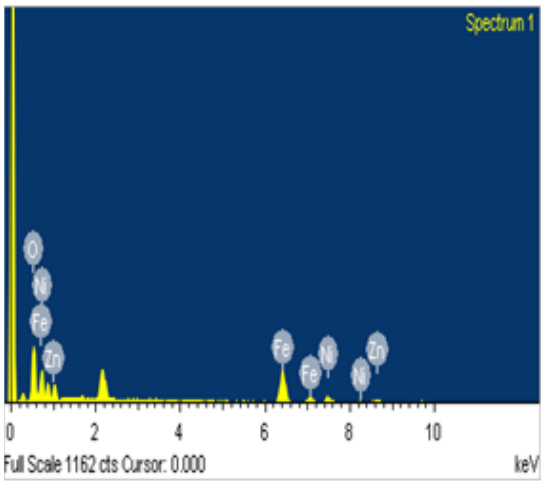

X=0.4

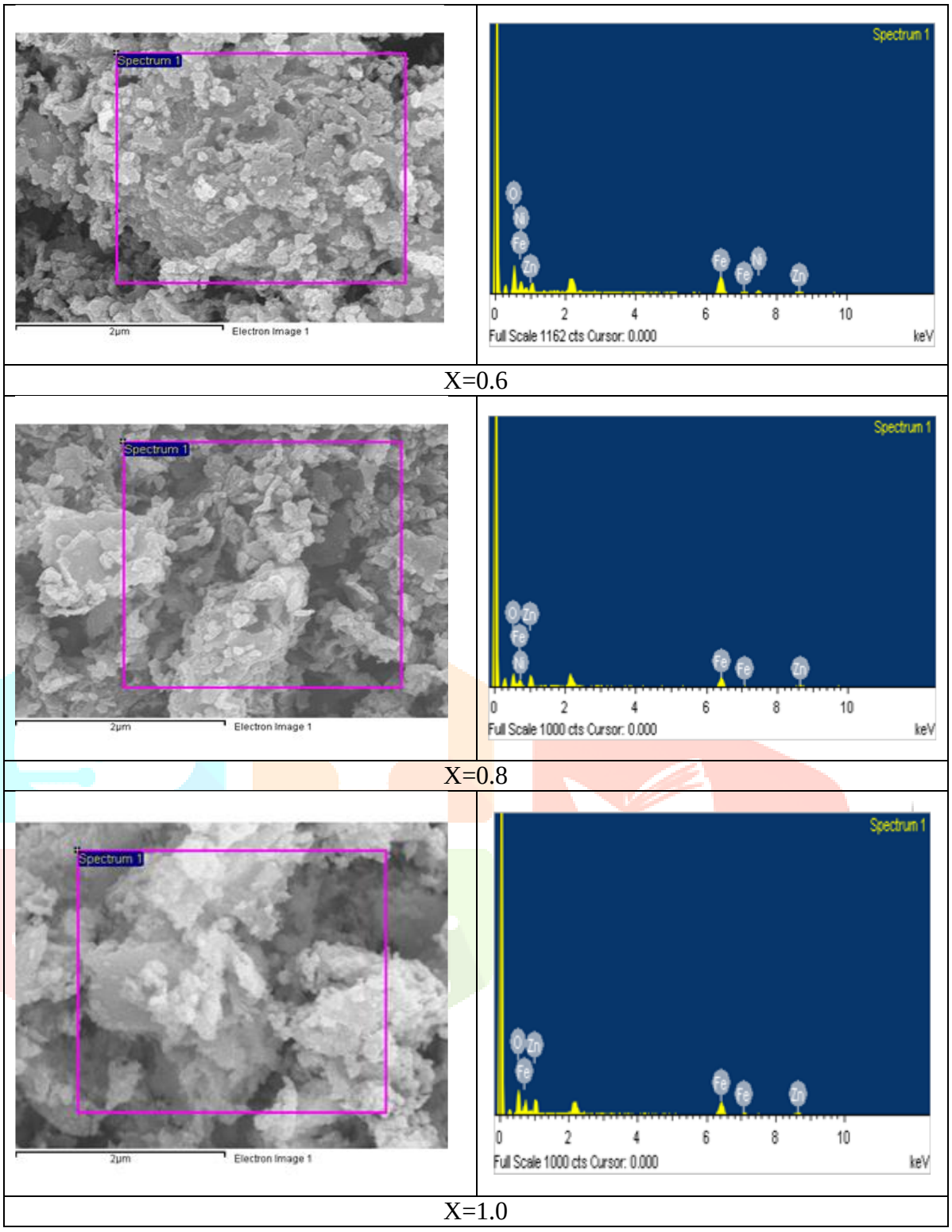

Fig.7. EDS spectra of $Ni_{1-x}Zn_xFe_2O_4$ nanoparticles (x=0.0, 0.2, 0.4, 0.6, 0.8, 1.0)

Table 2. EDS spectra analysis of $Ni_{1-x}Zn_xFe_2O_4$ nanoparticles (x=0.0, 0.2, 0.4, 0.6, 0.8, 1.0)

Zn^{2+} conc (x)	Element	Expected wt%	EDS wt%	Atomic wt%
0.0	**O K**	27.3	2.92	9.61
	Fe K	47.65	75.64	71.20
	Ni K	25.04	21.44	19.20
0.2	**O K**	27.14	20.9	47.36
	Fe K	47.38	51.31	34.65
	Ni K	19.91	22.96	14.74
	Zn K	5.54	5.63	3.25

0.4	**O K**	26.99	23.69	52.94
	Fe K	47.11	47.56	30.44
	Ni K	14.85	14.40	8.77
	Zn K	11.03	14.36	7.85
0.6	**O K**	26.84	28.38	48.19
	Fe K	46.85	49.20	33.33
	Ni K	9.84	13.26	8.55
	Zn K	16.45	17.16	9.93
0.8	**O K**	26.69	20.42	48.61
	Fe K	46.59	50.40	34.38
	Ni K	4.89	0.00	0.00
	Zn K	21.81	29.19	17.01
1.0	**O K**	26.54	26.65	57.27
	Fe K	46.33	46.23	28.46
	Zn K	27.12	27.12	14.26

5. Conclusion:

In this research work**,** $Ni_{1-x}Zn_xFe_2O_4$ nanoparticles (x=0.0, 0.2, 0.4, 0.6, 0.8, 1.0) were synthesized via sol-gel method. The effect of variation in Ni and Zn concentration morphological, structural, chemical performance was studied. The structural analysis of prepared samples were studied by powder XRD pattern that shows spinel structure with Fd-3m space group symmetry with lattice parameter increases with increase in Zn doping and also shift in the XRD peaks (311) and (400) towards lower angle occurs because of greater ionic radii of Zn^{2+} than that of Ni^{2+} and lattice strain and doping effects. Crystallite size for (311) plane observed between the 22nm to 29nm range.

The FESEM and EDS results showed the variation in surface microstructure of ferrites nanoparticles by changing concentration of Ni and Zn. The morphology of synthesized spinel ferrites changes with increase in Zn doping. At the higher doping concentration nanoparticles posse's agglomeration behaviour. On the other hand, EDS results confirm presence of expected elements such as Ni, Zn, O, Fe in the samples along with atomic % and weight % with variation Doping concentration of Zn.

Acknowledgement: Author acknowledges Mahatma Jyotiba Phule Research and Training Institute (MAHAJYOTI), Maharashtra State for the Jr Research Fellowship to first author and Ahmednagar College, Ahilyanagar & CT Bora College Shirur for providing synthesis & characterization facility.

REFERENCES:

[1] Gatelytė, A., Jasaitis, D., Beganskienė, A., & Kareiva, A. (2011). Sol-gel synthesis and characterization of selected transition metal nano-ferrites. *Materials science*, *17*(3), 302-307.

[2] Sharma, R., & Singhal, S. (2013). Structural, magnetic and electrical properties of zinc doped nickel ferrite and their application in photo catalytic degradation of methylene blue. *Physica B: Condensed Matter*, *414*, 83-90.

[3] Nguyen, L. T., Nguyen, H. T., Le, T. H., Nguyen, L. T., Nguyen, H. Q., Pham, T. T., ... & Tran, T. V. (2021). Enhanced photocatalytic activity of spherical Nd3+ substituted ZnFe2O4 nanoparticles. *Materials*, *14*(8), 2054.

[4] Valenzuela, R. (2012). Novel applications of ferrites. *Physics Research International*, *2012*(1), 591839.

[5] Job, A. E., de Siqueira, A. F., Danna, C. S., Bellucci, F. S., Cabrera, F. C., & Silva, L. E. K. (2014). Utilization of Composites and Nanocomposites Based on Natural Rubber and Ceramic Nanoparticles as Control Agents for Leishmania braziliensis. *Leishmaniasis-Trends in Epidemiology, Diagnosis and Treatment*.

[6] Atif, M. (2019). Synthesis and temperature dependent magnetic properties of nanocrystalline Ni 0.5 Zn 0.5 Fe 2 O 4 ferrites. *Materials Research Express*, *6*(7), 076104.
[7] Yu, Q., Su, Y., Tursun, R., & Zhang, J. (2019). Synthesis and characterization of low density porous nickel zinc ferrites. *RSC advances*, *9*(23), 13173-13181.
[8] Galal, A., Sadek, O., Soliman, M., Ebrahim, S., & Anas, M. (2021). Synthesis of nanosized nickel zinc ferrite using electric arc furnace dust and ferrous pickle liquor. *Scientific Reports*, *11*(1), 20170.
[9] Deshmukh, S. S., Humbe, A. V., Kumar, A., Dorik, R. G., & Jadhav, K. M. (2017). Urea assisted synthesis of Ni1− xZnxFe2O4 (0≤ x≤ 0.8): Magnetic and Mössbauer investigations. *Journal of Alloys and Compounds*, *704*, 227-236.
[10] Dumitrescu, A. M., Samoila, P. M., Nica, V., Doroftei, F., Iordan, A. R., & Palamaru, M. N. (2013). Study of the chelating/fuel agents influence on NiFe2O4 samples with potential catalytic properties. *Powder technology*, *243*, 9-17.
[11] Bhagwat, V. R., Humbe, A. V., More, S. D., & Jadhav, K. M. (2019). Sol-gel auto combustion synthesis and characterizations of cobalt ferrite nanoparticles: Different fuels approach. *Materials Science and Engineering: B*, *248*, 114388.
[12] Shoaib-ur-Rehman, M., Javaid, Z., Asghar, I., Azam, M., Shukrullah, S., Iqbal, F., ... & Naz, M. Y. (2020, May). Photo-catalytic response of zinc-doped nickel ferrite nanoparticles for removal of chromium from industrial wastewater. In *IOP Conference Series: Materials Science and Engineering* (Vol. 863, No. 1, p. 012017). IOP Publishing.
[13] Singhal, S., Namgyal, T., Bansal, S., & Chandra, K. (2010). Effect of Zn substitution on the magnetic properties of cobalt ferrite nano particles prepared via sol-gel route. *Journal of Electromagnetic Analysis and Applications*, *2010*.
[14] Chikazumi, S. (1959) Physics of Magnetism. Wiley, New York, 187.
[15] Hasan, S., & Azhdar, B. (2022). Synthesis of Nickel-Zinc Ferrite Nanoparticles by the Sol-Gel Auto-Combustion Method: Study of Crystal Structural, Cation Distribution, and Magnetic Properties. Advances in Condensed Matter Physics, 2022(1), 4603855